Research article

Improvement of digital Gabor holographic microscopy using a lens in plankton studies ☆

Yaumel C. Arias-Sosa [a,*], Gelaysi Moreno-Vega [b,c], Rubens M. Lopes [c], José-Luis Valin-Rivera [d], Meylí Valin-Fernández [e], Edison Gonçalves [f], Jorge O. Ricardo-Pérez [a]

[a] *Physics Department, Faculty of Natural and Exact Sciences, Universidad de Oriente, Santiago de Cuba, Cuba*
[b] *Physics Department, Higher Institute for Mining-Metallurgical, Moa, Holguín, Cuba*
[c] *Oceanographic Institute, University of São Pablo, São Pablo, Brazil*
[d] *Pontifícia Universidad Católica de Valparaíso, Escuela de Ingeniería Mecánica, Valparaíso, Chile*
[e] *Department of Mechanical Engineering (DIM), Faculty of Engineering (FI), University of Concepción, Chile*
[f] *Departamento de Mecatrônica e Sistemas Mecânicos, Escola Politécnica da Universidade de São Paulo (USP), São Paulo, SP, Brazil*

ARTICLE INFO

ABSTRACT

This work utilizes a Gabor Holographic Optical Scheme integrated with a microscope objective and a thin convex plane lens. This bi-telecentric lens system corrects spherical aberration from the objective, maintains consistent magnification across various reconstruction distances, and ensures a plane incidence on CMOS. Depending on the focal lengths of the objective and lens, the final image can be enlarged or reduced compared to the classic Gabor system, resulting in high-quality reconstructed phase images without spherical aberration. This setup was employed to capture phase distribution and intensity images of planktonic objects, such as copepods, achieving superior image quality.

1. Introduction

Digital Gabor Holographic Microscopy (DGHM) is a non-invasive optical technique typically used to study marine plankton. This technique enables the examination of large sample volumes while accurately preserving the positioning of individual particles [1]. Numerous studies have employed the reconstructed intensity contrast image obtained from Gabor configurations to determine characteristics such as specimen trajectories, movement speed, the number of specimens per unit volume, and spatial distribution based on depth in the seabed [2–4]. One of the most effective configurations for Gabor holographic techniques involves the use of a microscope objective to magnify the hologram captured in the CCD or CMOS camera [5].

The function of Microscope Objective (MO) placed on one of the arms of a Mach-Zehnder interferometer was analyzed [6], which generates spherical aberrations in the object beam. It is essential to correct this aberration to achieve a faithful phase contrast image
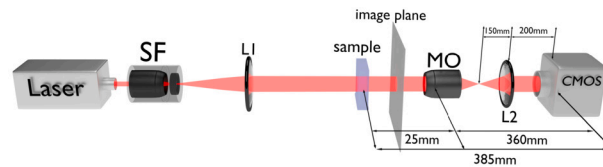
Fig. 1. Schematic representation of the experimental setup used.

in relation to the object, especially when using an off-axis scheme with a plane reference beam. In their work, they presented two new concepts for digital holography. The first one was the digital reference wave, which compensates for the role of the reference wave in an off-axis setup. The second concept was the digital phase mask, which compensates for the wavefront deformation caused by using a MO. Both of these concepts are defined numerically as arrays of complex numbers that are computed using phase reconstruction parameters. These parameters must be accurately defined to ensure that the computed data closely matches their experimental counterparts. This approach enables the reconstruction of absolute phase using a single hologram acquisition. These ideas were introduced by Cuche et al. in their paper [6].

To avoid this gauging problems, Ferraro et al. [7] proposed the use of a reference hologram, taken in a flat part of the sample, and a subtraction procedure for aberration compensation. While this simple technique is effective when parasitic conditions such as vibrations and drifts are well-managed, it is generally inadequate for providing accurate measurements in many situations and is therefore unsuitable for most practical applications. Additionally, the information needed for calculating the sample field is larger than what is typically required.

Colomb et al. describe a method in their paper [8] that corrects phase aberrations in Digital Holographic Microscopy (DHM) by computing a polynomial phase mask from the hologram itself. Another approach to address this issue is outlined in the reference [9], in which simultaneous dual-wavelength digital holography is employed to increase the range at which unambiguous phase imaging can be performed. This technique achieves nanometer-scale axial resolution.

The DHM has been notably improved by the recent introduction of Convolutional Neural Networks (CNNs). CNNs, a facet of deep learning technology, have the ability to perform end-to-end digital holographic reconstruction at in-line DHM, as well as completing phase aberration compensation in off-axis DHM [10]. These techniques require prior training with several samples that have certain similarities. For our case, where there is a large number of plankton species and significant morphometric diversity, performing this task is very difficult.

Several approaches for correcting aberrations in Digital Holography Microscopy have been developed and applied. Many of these methods are numerical techniques, limited to measuring thin and sparse objects such as living cells or thin lenses, where object phases are considered negligible in the reconstructed unwrapped phase map, or using a beam with a different wavelength (physical methods) [8,11–15]. To our knowledge, there are no reports on the use of our proposed optical method, which utilize a single beam and capture to address aberration issues. Our method achieves a constant magnification for all reconstruction distances while enhancing the quality of reconstructed images.

The aim of this work is to use a lens to correct aberrations, maintain optical field magnification, and ensure plane wave incidence on the CMOS camera for Digital Gabor Holography Microscopy (DGHM). We achieve this by placing a plane convex lens between the microscope objective (MO) and CMOS camera, aligning it with the focal image of the MO and the object focus of the corrector lens. This arrangement ensures a plane wavefront reaches the CMOS camera, compensating for the MO's influence and enhancing image reconstruction quality. The configuration of the lens and MO resembles an inverted bitelecentric lens system. This experimental setup, aimed at improving reconstruction quality using a lens, has not been previously reported in the literature, to the best of our knowledge.

2. Experimental setup

Fig. 1 shows an schematic representation of the experimental optical setup used in this work. It consists on a CUBE 660 nm 60 mW Laser System, Circular Beam. Where SF is a Spatial Filter, Compact, Five-Axis, XY $x\theta y\theta$ 100TPI, Z 80TPI, model 910A from Newport. $L1$ lens with focal distance $f = 150$ mm for SF output light beam parallelism correction. A laboratory cuvette with the "sample". MO is an infinite corrected plane field microscope objective UPLAN FLN $4x/0.13$, from Olympus. CMOS is a Basler acA 2000 165-uc camera with pixel size 5.50 μm by 5.50 μm with a maximum resolution of 2040×1086 pixels and $L2$ is the second lens for MO output hologram parallelism correction and aberration corrections, with focal distance $f^* = 150$ mm.

The camera's exposure time was set to 15 milliseconds to ensure proper illumination at the image plane, resulting in a capture frequency of 94 Hz, without the use of any neutral attenuator in the optical beam path. The camera can be controlled by mean of the `HoloDIG v1.1` (ad hoc software see Subsection 2.1), and through the Pylon software. A linear scale of 5 mm with 50 μm division value of `THORLABS`, and an `USAF 1951` test target are used for calibration. All holograms were captured, processed, reconstructed and displayed using the `HoloDIG v1.1`.

2.1. HoloDIG v1.1 software

The software has been in development for many years using MatLab, and its latest version has been updated to MatLab 2020a. Utilizing HoloDIG v1.1 software, users can effectively capture holograms, reconstruct images and calculate amplitude field distri-
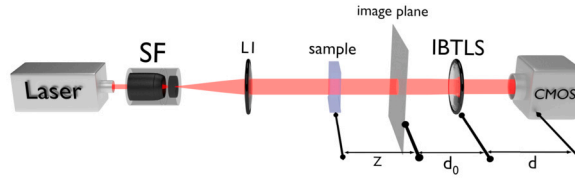
Fig. 2. Schematic representation of the experimental setup used considering the MO and corrector lens as a thin lens. IBTLS denotes the Inverted Bitelecentric Lens System.

bution. With its user-friendly interface and advanced features, HoloDIG v1.1 has continuously proven to be a reliable tool for the analysis of holographic data. The program allows to control the holograms or video hologram capture, the reconstruction process of the optical field of the amplitude image and other operations, such as: find the best reconstructing distance z_i in dependence of the focus metric used, filtering, unwrapping algorithms, ROI selection, calibration and 3D representation using phase images, etc.

The minimum requirements for the HoloDIG v1.1 Software are:

- Processor: A CPU manufactured by Intel or AMD with a 64-bit architecture and four logical cores, which also supports the AVX2 instruction set.
- RAM: 8 GB.
- Hard Disk Space: 20 GB of HDD space.
- Graphics: There are no specific graphics card demanded. Rather, a hardware-accelerated graphics card, which supports OpenGL 3.3 and has at least 1 GB of GPU memory is needed. Additionally, the minimum resolution requirement is 1024×768.
- Operative system: Windows 10x64 (version 1709 or later).
- Additionally requires: Java Runtime Environment (JRE) version 11.

The `HoloDIG v1.1` has been used for the capture, processing and reconstruction of the holograms in our recent works [16–18].

3. Basic principles and methods

A plane monochromatic wave originates from SF and undergoes diffraction in the sample. The magnified image, produced by the inverted telescope system, is projected onto the CMOS camera, where the magnified Gabor hologram is recorded. The experimental setup used in this work resembles a traditional Digital Gabor Holography configuration, with the addition of the bi-telecentric system lens (refer to Fig. 1). The Gabor hologram of an unfocused object is captured by the sensor, which is then used to reconstruct the object phase and amplitude contrast images, these are reconstructed at the distance determined by the refocusing algorithms. This Gabor hologram is an interference pattern that arises due to diffraction at the object and reference plane wave.

3.1. Digital Gabor holographic microscopy

The method used to compute the magnified hologram was developed by Sheng et al. [19] and has been applied in previous studies [2,20,21]. In their work, Sheng et al. [19] recorded magnified holograms by focusing a microscope objective (MO) on a plane located near the sample volume. The optical field generated by hologram at the image plane $U(x, y; z)$ can be computed by mean of Eq. (1):

$$
\begin{aligned}
U(x, y; z) = & \frac{1}{M} U_H\left(-\frac{x}{M}, -\frac{y}{M}\right) \times \\
& \exp\left[\frac{jk}{2M^2 d_0}\left(x^2 + y^2\right)\right] \times \exp\left[\frac{jk}{2d}\left(x_0^2 + y_0^2\right)\right]
\end{aligned}
\tag{1}
$$

where U_H is field at hologram plane, in the CMOS Camera, $j = \sqrt{-1}$, $k = 2\pi/\lambda$, λ is the wavelength, d_0 is the distance between image plane and the MO, d is the distance between MO and the CMOS Camera and $M = d/d_0$ is the Magnification (see Fig. 2). The field intensity at the image plane is:

$$
I(x, y) = \frac{1}{M^2} U_H\left(-\frac{x}{M}, -\frac{y}{M}\right) U_H^*\left(-\frac{x}{M}, -\frac{y}{M}\right)
\tag{2}
$$

The magnified wave field can be reconstructed numerically using different reconstruction methods (Fresnel Transform, Huygens Convolution, Angular Spectrum, etc). According to Kim et al. [5], these methods have different benefits and drawbacks despite sometimes being called by ambiguous or inconsistent names. In this work, the Angular Spectrum Method (ASM) has been utilized as it is based on the propagation of plane waves that conserves the pixel size with increasing reconstruction distance. This property makes ASM ideal for our experimental setup as it does not have any distance limitations. In summary, ASM has been chosen due to its ability to maintain high-quality image resolution over various distances, providing an efficient and reliable tool for our experimental analysis [22].

3.2. Spectrum angular method

The field $\varphi(x, y; z)$ is digitized and computed using the ASM, this method has been explained and used in several works [5,23–26]. The reference used for our work is [27], because in this book is presented even the code implementation.

$$\varphi(x', y'; z) = \mathfrak{F}^{-1} \left\{ \mathfrak{F} \left\{ U_h \left(x', y' \right) \right\} \times H(k_{x'}, k_{y'}; z) \right\} \tag{3}$$

where $H(k_{x'}, k_{y'}; z)$ is the spatial frequency transfer function:

$$H(k_{x'}, k_{y'}; z) = \exp \left[-jk_0 z \sqrt{\left(1 - \frac{k_x'^2}{k_0^2} - \frac{k_y'^2}{k_0^2} \right)} \right] \tag{4}$$

3.3. Spectrum angular method with magnification

By using an IBTLS, replacing $x' = x/M$ and $y' = y/M$, the Angular Spectrum Method is expressed as follows:

$$\varphi_M(x, y; z) = \mathfrak{F}^{-1} \left\{ \mathfrak{F} \left\{ U_h \left(\frac{x}{M}, \frac{y}{M} \right) \right\} H_M(k_x M, k_y M; z) \right\} \tag{5}$$

where $H_M(k_x M, k_y M; z)$ is the modified spatial frequency transfer function:

$$H_M(k_x M, k_y M; z) = \exp \left[-jz \sqrt{\left(k_0^2 - (k_x^2 + k_y^2) M^2 \right)} \right] \tag{6}$$

where z is the distance between image plane and the reconstructed plane.

It's crucial to maintain the distance between the reconstructed image and the image plane equal to the distance between the original plane in the sample volume and the object plane of the microscope, provided the wavelength remains constant for both recording and reconstruction.

For computation purposes, the Inverted Bi-telecentric Lens System (IBTLS) can be treated as a lens with consistent magnification across the system, which is $M = d/d_0$ see Fig. 1. This magnification is calculated using the equivalence between d/d_0 and h/h_0, where h and h_0 are the sizes of $R1L3S1 - 10mm$ in image plane and CMOS plane respectively, then $M = 4.29$.

3.4. Detection of focal plane

Determining the best focal plane is crucial in holographic reconstruction, especially for dynamic samples like living organisms. Many refocusing criteria have been compared in the literature [28–33], each with its advantages and disadvantages depending on the sample and experimental setup. These criteria often focus on optimizing image contrast for precise determination of the object's focal plane. Our study has shown that the F_{GINI} and F_{FSL} refocusing criteria provide the best results. The first one is based on a new sparsity measurement coefficient, called GINI's index, which has been proposed for digital holograms and tested for microscopic setups [34].

3.4.1. GINI index as refocusing criterion (F_{GINI})

The Gini index evaluates how much the allocation of income or consumption varies between households or individuals in an economy, compared to a completely equal distribution. It can be calculated using the following formula:

$$F_{GINI} = 1 - 2 \sum_{k=1}^{N} \frac{a_k(z)}{\|\mathbf{c}(z)\|_1} \left(\frac{N - k + 0.5}{N} \right) \tag{7}$$

where $\mathbf{a} = \text{vec}\{A\}$, $\mathbf{c} = \text{vec}\{C\}$, and the operator $\text{vec}\{\cdot\}$ create a column vector from a matrix, $\|\cdot\|$ is the l_1 norm, and a_k for $k = 1, \ldots, N$ are the sorted entries of vector a in increasing order. This index can be used as refocusing metric. The second one is a weighted Fourier Spectral Focus Measure.

3.4.2. The weighted spectral method (F_{FSL})

This measure gauges the sharpness of an image by analyzing its spatial frequency content. The logarithmically weighted power spectrum is used to achieve the following equation as outlined in Fonseca et al. [29]:

$$F_{FSL} = \sum_{m=1}^{M} \sum_{n=1}^{N} \log\{1 + [\mathcal{F}_F g(m, n)]\} \tag{8}$$

in the equation, $\mathcal{F}_F g(m, n)$ indicates the Fourier transform of the amplitude distribution. In DHM, specifically when employing an off-axis setup, a high-pass filter is normally employed prior to the Fourier transform. However, the version used in this particular study is unfiltered.
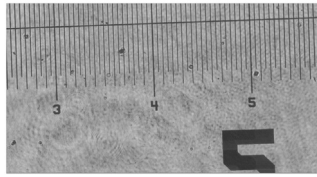
Fig. 3. R1L3S1P-10mm Stage Micrometer, used for calibration, sample in the focal plane.

(a) Hologram$_1$

(b) Hologram$_2$

(c) Focus metric$_1$

(d) Focus metric$_2$

(e) Recontructed image$_1$
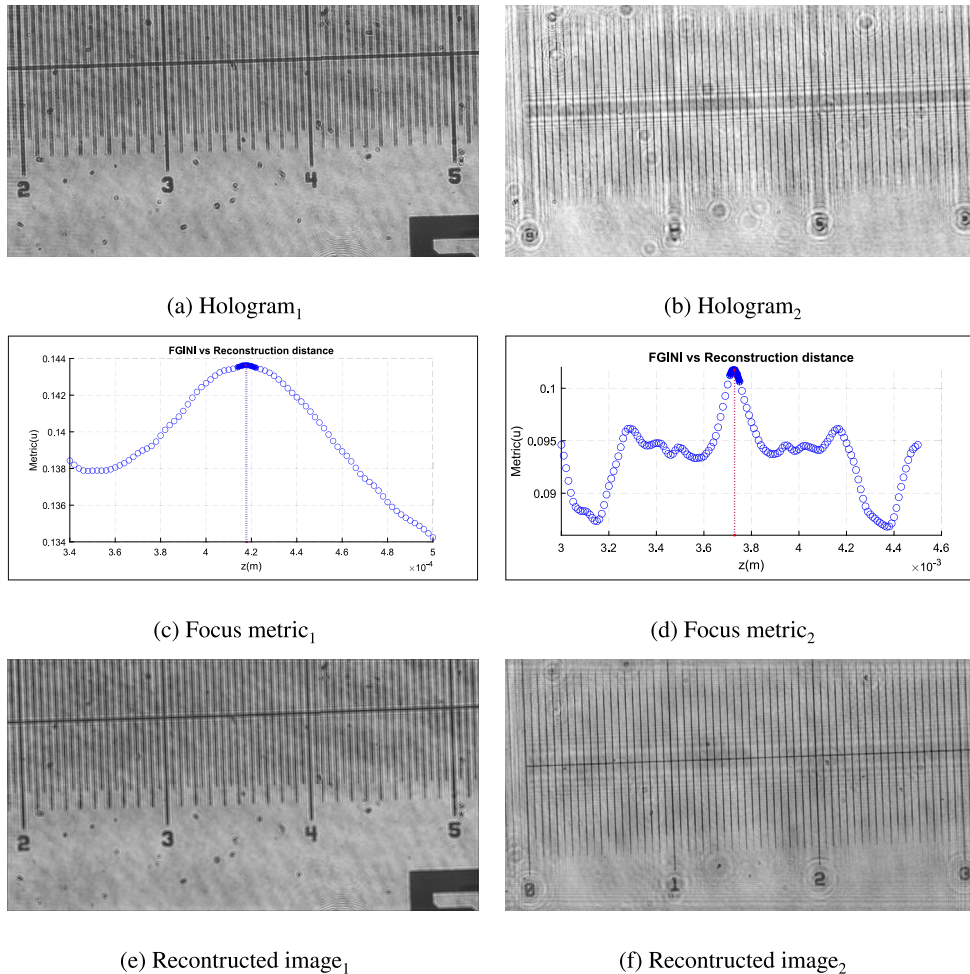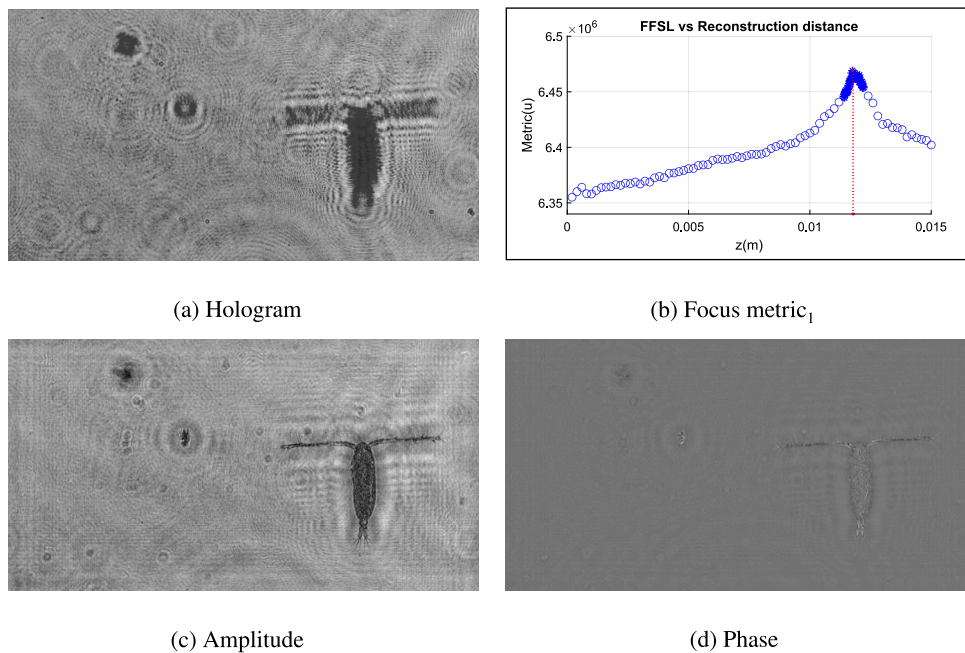

(f) Recontructed image$_2$

Fig. 4. (a) and (b) R1L3S1P-10mm Stage Micrometer, hologram with the sample shifted out of focus 0.4 mm and 3.7 mm respectively, (c) and (d) focus metric curves vs distance of reconstruction using F_{GINI} for each hologram, (e) and (f) the reconstructed amplitude contrast images for holograms 1 and 2 respectively.

3.5. Calibration and samples

The R1L3S1P-10mm (Fig. 3) Stage Micrometer with 50 μm Divisions ($3'' \times 1''$), from THORLABS was used for experimental setup calibration.

For checking the reconstruction distance quality, micro-ruler R1L3S1P-10mm was shifted out of focus a known distance from 0 mm (object in focus) to 5 mm with step 0.1 mm. Figs. 4a and 4b show two of the captured holograms of R1L3S1P-10mm Stage Micrometer, in this case, the sample was shifted out of focus by 0.4 mm and 3.7 mm, respectively. Figs. 4c and 4d plot the focus metric curves against the distance of reconstruction for each hologram, as calculated using F_{GINI}. Finally, Figs. 4e and 4f portray the reconstructed amplitude contrast images for hologram 1 and 2, respectively.

Live organisms were collected at the Flamengo Inlet, located at Ubatuba, Brazil ($23°31'20''$S, $45°4'60''$W) through gentle vertical tows with a conical plankton net from 10 m depth to the surface and immediately brought to a controlled temperature room in the laboratory. After gentle homogenization, different aliquots of varying volumes were removed from the original sample with a large diameter pipette to identify and separate the organisms on a Nikon SMZ800 stereo-microscope. Individuals from selected species

(a) Hologram

(b) Focus metric$_1$

(c) Amplitude

(d) Phase

Fig. 5. (a) Hologram of a sample containing planktonic organisms of different sizes, (b) Focus metric curve vs distance of reconstruction using F_{FSL}, (c) and (d) the reconstructed amplitude and phase contrast images respectively. The in-focus organism is a juvenile copepodite of *Acartia lilljeborgii*.

(*Acartia lilljeborgii* and *Temora turbinata*) were transferred to a cubic glass container measuring 32.5 mm × 45 mm and 12.5 mm in z direction, and holograms were captured at 94 frames per second while the animals were swimming freely.

The optical system magnification (M) was computed using the R1L3S1P-10mm field of view distance, from Fig. 3 it is 3.25 m, and the CMOS sensor size in the same direction is 11.3 mm, whereby $M = 11.3$ mm$/3.25$ mm $= 3.47$ this is equivalent to $M = d/d_0$. Thanks to the use of IBTLS this magnification is the same for all reconstruction distances the object position, as long as the same lens and objective positions are maintained.

4. Experimental results and discussions

Video-holograms of planktonic objects were recorded as they moved freely in seawater. These holograms were used to calculate the reconstruction distance for each moment of movement and reconstruct the corresponding image. In the typical Gabor hologram capture, the reference beam reaches the CMOS camera in a parallel manner. However, in the DGHM configuration without the L2 lens, beams passing through the MO from objects outside the image plane generate divergence.

The distribution of values obtained for the focus criterion F_{FSL} in relation to the reconstruction distance showed an absolute maximum in the position of best focus in all cases analyzed (Figs. 5b, 6b and 7b), which is associated with the position where the body of the copepods is fully or partially in focus.

The focus function was applied to all holograms with different live zooplanktonic organisms swimming freely in the aquarium to calculate the position of the focal plane, three examples of these holograms are shown (Figs. 5b, 6b and 7b). It is important to note that the selected organisms have complex 3D morphological structures of different sizes and shapes, such as swimming legs, antennas, and tentacles, which can be oriented in different reconstruction planes, making the reconstruction process and focal position calculation difficult. Figs. 5c and 5d show the reconstructed phase and amplitude contrast images of hologram (Fig. 5a) at the refocus distance of 11.75 mm. The reconstructed images exhibit excellent quality, allowing for clear identification of the organisms' morphological traits.

The L2 lens was positioned between the MO and the CMOS sensor to correct the divergence of the holographic beams, ensuring that the reference beam returns to parallel. The CMOS was aligned to focus the image of an object from the MO's image plane onto its sensor. The sample can be positioned before or after the image plane for recording as a Gabor hologram on the CMOS.

In the example depicted in Fig. 6, the copepod *Temora turbinata* is observed compared to the object in Fig. 5. Figs. 6c and 6d display the phase and amplitude contrast images reconstructed from the hologram in Fig. 6a at a refocus distance of 11.21 mm, as indicated by the peak of the focus metric curve in Fig. 6b. This refocus distance presents a challenge in capturing a complete hologram of the object without edge aberrations. The inclusion of L2 in Digital Gabor Holographic Microscopy (DGHM) enables high-quality reconstructions of objects occupying a greater number of pixels in the hologram, which would be unattainable with traditional DGHM lacking L2.

Fig. 7 depicts a calanoid copepod. Figs. 7c and 7d represent the reconstructed phase and amplitude contrast images from the hologram in Fig. 7a, taken at a refocus distance of 11.38 mm. Additionally, Fig. 7e provides a 3D view of a rectangular section from

(a) Hologram

(b) Focus metric₁
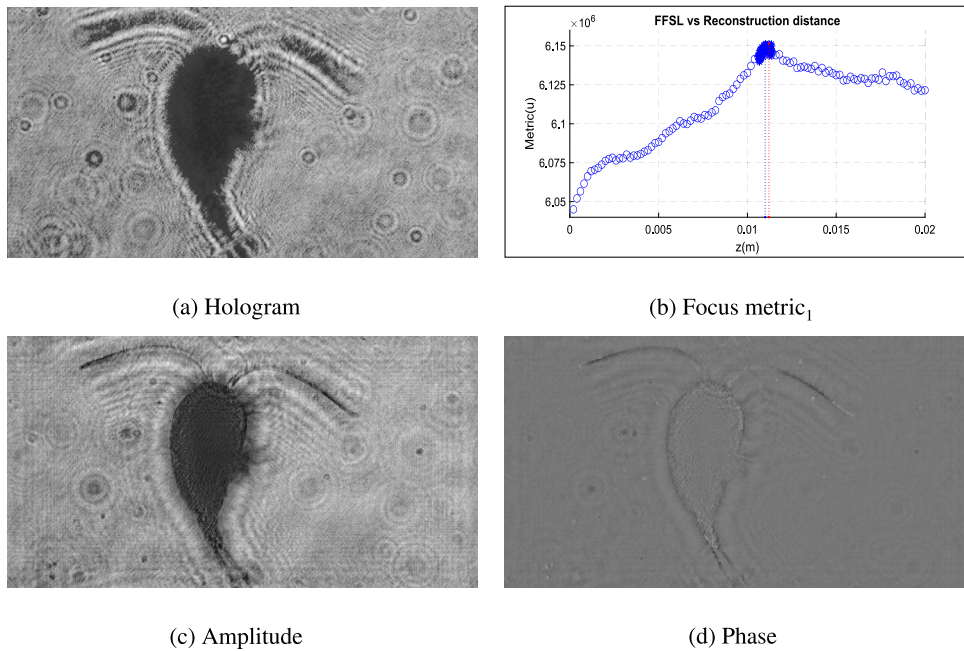
(c) Amplitude

(d) Phase

Fig. 6. (a) Hologram with the sample, (b) Focus metric curve vs distance of reconstruction using F_{FSL}, (c) and (d) the reconstructed amplitude and phase contrast images respectively. The organism in focus corresponds to the species *Temora turbinata*.

the phase contrast image, highlighted by dashed red lines in 7d. At this refocus distance, a high-quality reconstructed phase contrast image is evident. Notably, the antennae exhibit a significant phase change, possibly due to their composition with substances of a higher refractive index or larger dimensions along the z-axis of our reference system.

The reduced transparency of this organism may contribute to minimal transmitted light passing through, impacting the quality of phase contrast imaging when dealing with non-transparent organisms. This limitation stems from classical DHGM and is present in our proposed experimental setup. To address this, it is advisable to consider using reflection DHGM instead of transmission DHGM. Another notable limitation is the organism size, constrained by the microscope objective's resolution. The minimum size should roughly match the microscope objective resolution, while the maximum size should align with the sensor's dimensions divided by the magnification. In our case, this translates to 4 mm diagonally, corresponding to 12.8 mm/3.25 mm.

Fig. 8 shows a comparison between the new experimental setup using the IBTLS (with L2) and a classical DHGM system (without L2), with the aim of highlighting spherical correction. Figs. 8a and 8b shows the reconstructions of the phase-contrast images from the holograms obtained for sample R1l3S1P-10mm, using the IBTLS and classical DHGM configurations respectively, which at first glance appear to be very similar. However, if it is observed the regions marked with red lines in the phase-contrast images carefully, the presence of spherical aberrations can be observed in the case of the DHGM configuration, while for the IBTLS case, these aberrations are practically eliminated. In the Figs. 8c and 8d, the regions of interest were zoomed in to show with greater clarity what was explained before.

In addition, Figs. 8e and 8f show an axial scan in the zoomed-in figures of the two experimental setups. It can be observed that for the classical DHGM case, there is a high influence of spherical aberrations from 300 micrometers to 700 micrometers, Fig. 8f. Due to this, identifying the local minima corresponding to the division lines in the R1LS31P-10mm micro-ruler shard in this region is challenging. Holograms of a micro-ruler are used to illustrate the correction of spherical aberrations, because it is almost impossible to obtain two similar holograms of a live plankton sample with the two configurations. One of the main advantages of the bi-telecentric lens system is the correction of spherical aberrations, which has been previously reported in [35] and exemplified in Fig. 8. In this system, the quadratic phase factor introduced by the microscopic object is minimized with L2 placed correctly.

Another important point to highlight is that the lens L2 must be properly positioned, and the focus position must be adjusted with a micrometer scale (so that the focus of the MO and the lens coincide as shown in Fig. 1. If these conditions are not met, the lens will fail to achieve its three fundamental objectives. The wavefront exiting L2 will not be flat, leading to inconsistent magnification across reconstruction distances, inadequate aberration correction, and non-planar sensor incidence. Plane incidence is crucial for hologram reconstructions, as utilized in most publications in this field due to the reconstruction models relying on a flat wave for hologram reconstruction.

5. Conclusions

Based on the initial assumptions and the results presented, it can be concluded that incorporating IBTLS into DGMH reduces the impact of spherical aberrations, ensures a consistent total magnification, and improves the quality of reconstructed images.

(a) Hologram

(b) Focus metric$_1$

(c) Amplitude
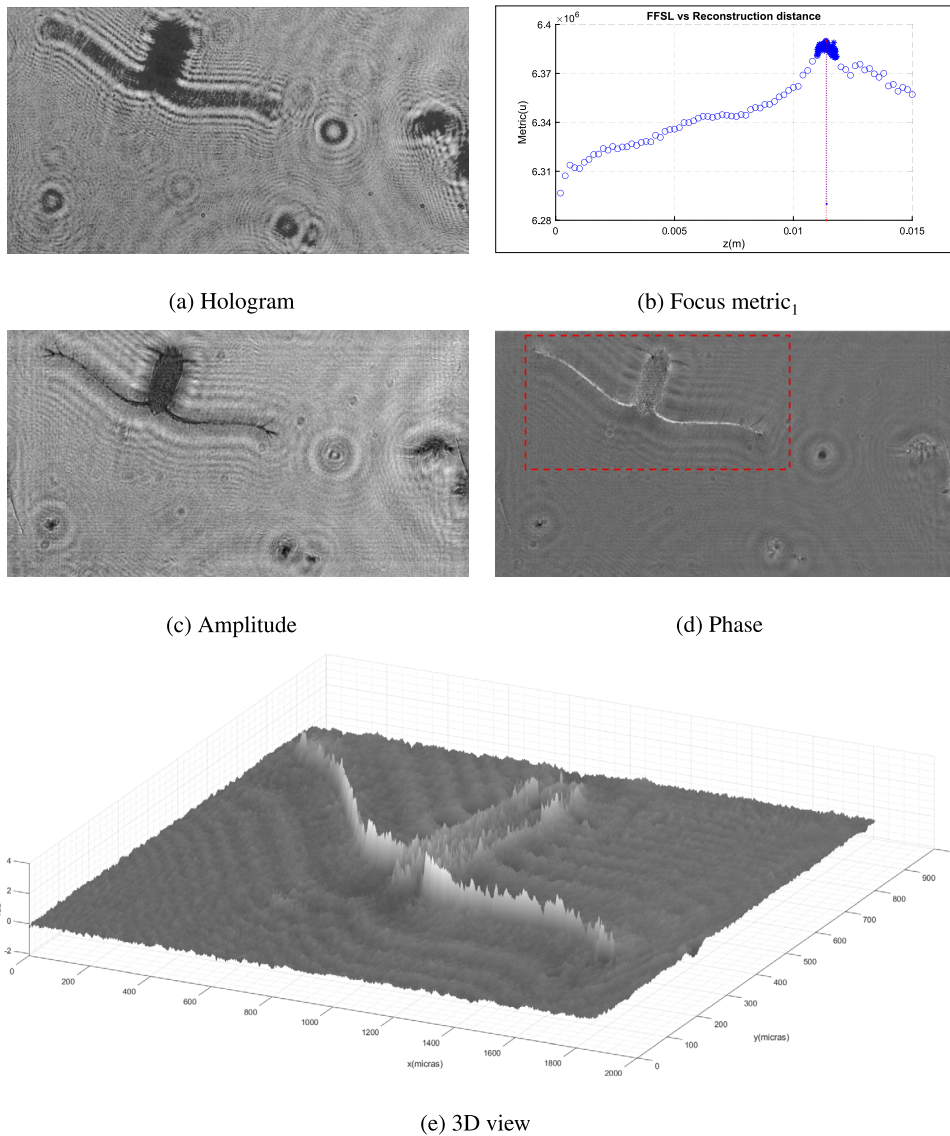
(d) Phase

(e) 3D view

Fig. 7. (a) Hologram of planktonic organisms of different sizes, (b) Focus metric curve vs distance of reconstruction using F_{FSL}, (c) and (d) the reconstructed distribution amplitude and phase contrast images respectively, (e) 3D view of a crop d, which is shown with discontinue red lines. The organism in focus corresponds to the species *Temora turbinata*.

Depending on the size of the marine plankton object under study, the system's magnification can be adjusted to achieve the optimal image quality, facilitating the calculation of dynamic movement parameters if needed.

In this study, a new experimental configuration using the IBTLS setup to enhance DGHM with a lens is proposed. The effectiveness of this approach is demonstrated by utilizing a Gabor Holographic Optical Scheme with a built-in microscope objective and a thin convex plane lens, creating a bi-telecentric lens system. This system is versatile, capable of enlarging or reducing the final image, resulting in a high-quality reconstructed phase image free of spherical aberration. By applying this system, high-quality images of planktonic organisms such as live copepods have been captured, offering valuable insights for marine biology research.

CRediT authorship contribution statement

Yaumel C. Arias-Sosa: Writing – review & editing, Writing – original draft, Validation, Software, Methodology, Investigation, Formal analysis, Conceptualization. **Gelaysi Moreno-Vega:** Writing – original draft, Data curation. **Rubens M. Lopes:** Resources, Project administration, Methodology. **José-Luis Valin-Rivera:** Writing – original draft, Resources, Methodology, Funding acquisition, Conceptualization. **Meylí Valin-Fernández:** Writing – original draft, Investigation, Funding acquisition, Conceptualization. **Edison Gonçalves:** Investigation, Funding acquisition, Conceptualization. **Jorge O. Ricardo-Pérez:** Writing – original draft, Visualization, Validation, Project administration, Methodology, Investigation, Formal analysis, Data curation, Conceptualization.
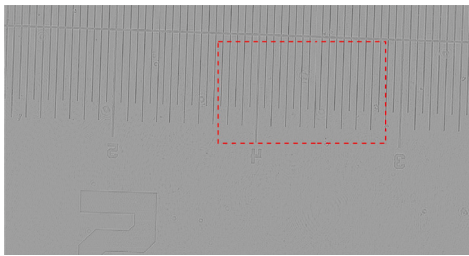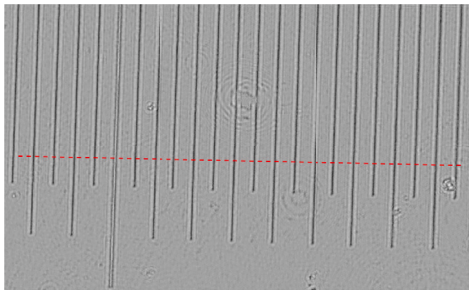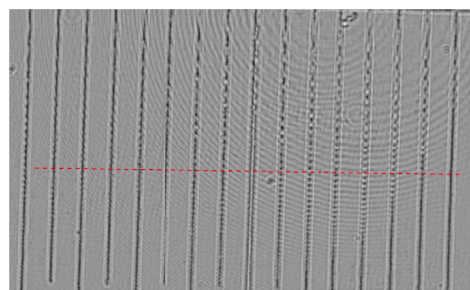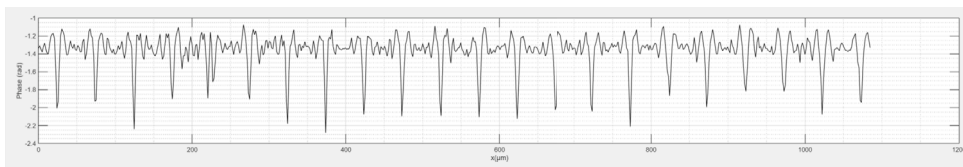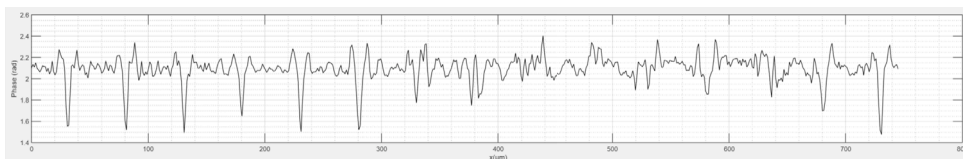
(a) Phase with L2
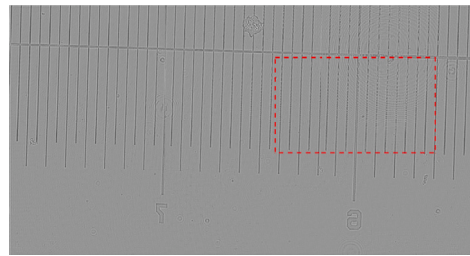
(b) Phase without L2

(c) Fig. 8a zoom

(d) Fig. 8b zoom

(e) Axial scanning in Fig. 8c

(f) Axial scanning in Fig. 8d

Fig. 8. (a) Phase contrast image of R1L3S1P-10mm Stage Micrometer hologram recorded using the IBTLS (with L2), (b) Phase contrast image of R1L3S1P-10mm Stage Micrometer hologram recorded using DHGM classic experimental setup (without L2), (c) and (d) the zoomed regions, which are enclosed by red discontinuous rectangle lines in a) and b) respectively, (e) and (f) Axial scanning of c) and d), which are shown with discontinuous red lines in their respective figures.

Declaration of competing interest

The authors declare that they have no known competing financial interests or personal relationships that could have appeared to influence the work reported in this paper.

References

[1] S. Tan, S. Wang, An approach for sensing marine plankton using digital holographic imaging, Optik 124 (2013) 6611–6614.
[2] J. Sheng, E. Malkiel, J. Katz, Using digital holographic microscopy for simultaneous measurements of 3D near wall velocity and wall shear stress in a turbulent boundary layer, Exp. Fluids 45 (2008) 1023–1035.
[3] E. Darakis, T. Khanam, A. Rajendran, V. Kariwala, T.J. Naughton, A.K. Asundi, Microparticle characterization using digital holography, Chem. Eng. Sci. 65 (2010) 1037–1044.
[4] A.B. Bochdansky, M.H. Jericho, G.J. Herndl, Development and deployment of a point-source digital inline holographic microscope for the study of plankton and particles to a depth of 6000 m, Limnol. Oceanogr., Methods 11 (2013) 28–40.
[5] M.K. Kim, Digital Holographic Microscopy: Principles, Techniques, and Applications, Springer Series in Optical Sciences, vol. 162, Springer, New York, 2011.
[6] E. Cuche, P. Marquet, C. Depeursinge, Simultaneous amplitude-contrast and quantitative phase-contrast microscopy by numerical reconstruction of Fresnel off-axis holograms, Appl. Opt. 38 (1999) 6994.

[7] P. Ferraro, S. De Nicola, A. Finizio, G. Coppola, S. Grilli, C. Magro, G. Pierattini, Compensation of the inherent wave front curvature in digital holographic coherent microscopy for quantitative phase-contrast imaging, Appl. Opt. 42 (2003) 1938.

[8] T. Colomb, E. Cuche, F. Charrière, J. Kühn, N. Aspert, F. Montfort, P. Marquet, C. Depeursinge, Automatic procedure for aberration compensation in digital holographic microscopy and applications to specimen shape compensation, Appl. Opt. 45 (2006) 851.

[9] A. Khmaladze, M. Kim, C.-M. Lo, Phase imaging of cells by simultaneous dual-wavelength reflection digital holography, Opt. Express 16 (2008) 10900–10911.

[10] S. Ma, R. Fang, Y. Luo, Q. Liu, S. Wang, X. Zhou, Phase-aberration compensation via deep learning in digital holographic microscopy, Meas. Sci. Technol. 32 (2021) 105203.

[11] C. Cho, B. Choi, H. Kang, S. Lee, Numerical twin image suppression by nonlinear segmentation mask in digital holography, Opt. Express 20 (2012) 22454.

[12] H. Cui, D. Wang, Y. Wang, J. Zhao, Y. Zhang, Phase aberration compensation by spectrum centering in digital holographic microscopy, Opt. Commun. 284 (2011) 4152–4155.

[13] J. Di, J. Zhao, W. Sun, H. Jiang, X. Yan, Phase aberration compensation of digital holographic microscopy based on least squares surface fitting, Opt. Commun. 282 (2009) 3873–3877.

[14] R.G. González-Acuña, H.A. Chaparro-Romo, General formula for bi-aspheric singlet lens design free of spherical aberration, Appl. Opt. 57 (2018) 9341.

[15] R.G. González-Acuña, M. Avendaño-Alejo, J.C. Gutiérrez-Vega, Singlet lens for generating aberration-free patterns on deformed surfaces, J. Opt. Soc. Am. A 36 (2019) 925.

[16] M. Frómeta, G. Moreno, J. Ricardo, Y. Arias, M. Muramatsu, L.F. Gomes, G. Palácios, F. Palácios, H. Velázquez, J.L. Valin, L. Ramirez Q, Optimized setup for integral refractive index direct determination applying digital holographic microscopy by reflection and transmission, Opt. Commun. 387 (2017) 252–256.

[17] G. Moreno, J.S. Ascaneo, J.O. Ricardo, L.T. De La Cruz, Y. Arias, J.R. Strickler, R.M. Lopes, A new focus detection criterion in holograms of planktonic organisms, Pattern Recognit. Lett. 138 (2020) 497–506.

[18] Y.C. Arias Sosa, G.M. Vega, J.L. Valin Rivera, R.M. Lopes, M.E. Planos Valenzuela, M.V. Fernández, E. Gonçalves, J.O. Ricardo Pérez, Alternative use of reflection spatial light modulator in phase shifting digital Gabor holography, Optik 233 (2021) 166609.

[19] J. Sheng, E. Malkiel, J. Katz, Digital holographic microscope for measuring three-dimensional particle distributions and motions, Appl. Opt. 45 (2006) 3893.

[20] J. Sheng, E. Malkiel, J. Katz, J. Adolf, R. Belas, A.R. Place, Digital holographic microscopy reveals prey-induced changes in swimming behavior of predatory dinoflagellates, Proc. Natl. Acad. Sci. 104 (2007) 17512–17517.

[21] J. Katz, J. Sheng, Applications of holography in fluid mechanics and particle dynamics, Annu. Rev. Fluid Mech. 42 (2010) 531–555.

[22] G. Wang, H. Wang, D. Wang, J. Xie, J. Zhao, Reconstruction of off-axis lensless Fourier transform digital holograms based on angular spectrum theory, Chengdu, China, 2007, p. 67234L, http://proceedings.spiedigitallibrary.org/proceeding.aspx?doi=10.1117/12.783649.

[23] T.M. Kreis, M. Adams, W.P.O. Jueptner, Methods of digital holography: a comparison, Munich, Germany, 1997, pp. 224–233, http://proceedings.spiedigitallibrary.org/proceeding.aspx?articleid=928168.

[24] T.M. Kreis, Frequency analysis of digital holography, Opt. Eng. 41 (2002) 771.

[25] S. De Nicola, A. Finizio, G. Pierattini, P. Ferraro, D. Alfieri, Angular spectrum method with correction of anamorphism for numerical reconstruction of digital holograms on tilted planes, Opt. Express 13 (2005) 9935.

[26] M. Özcan, M. Bayraktar, Digital holography image reconstruction methods, San Jose, CA, 2009, p. 72330B, http://proceedings.spiedigitallibrary.org/proceeding.aspx?doi=10.1117/12.808835.

[27] T.-C. Poon, J.-P. Liu, Introduction to Modern Digital Holography: With Matlab, Cambridge University Press, 2014.

[28] A. He, W. Xiao, F. Pan, Automatic focus determination through cosine and modified cosine score in digital holography, Opt. Eng. 56 (2017) 034103.

[29] E.S.R. Fonseca, P.T. Fiadeiro, M. Pereira, A. Pinheiro, Comparative analysis of autofocus functions in digital in-line phase-shifting holography, Appl. Opt. 55 (2016) 7663.

[30] P. Memmolo, L. Miccio, M. Paturzo, G.D. Caprio, G. Coppola, P.A. Netti, P. Ferraro, Recent advances in holographic 3D particle tracking, Adv. Opt. Photonics 7 (2015) 713.

[31] A. El Mallahi, F. Dubois, Dependency and precision of the refocusing criterion based on amplitude analysis in digital holographic microscopy, Opt. Express 19 (2011) 6684.

[32] S.K. Mohammed, L. Bouamama, D. Bahloul, P. Picart, Quality assessment of refocus criteria for particle imaging in digital off-axis holography, Appl. Opt. 56 (2017) F158–F166.

[33] H. Wang, Z. Dong, S. Wang, Y. Lou, Comparison of the refocus criteria for the phase, amplitude, and mixed objects in digital holography, Opt. Eng. 57 (2018) 054111.

[34] P. Memmolo, M. Paturzo, B. Javidi, P.A. Netti, P. Ferraro, Refocusing criterion via sparsity measurements in digital holography, Opt. Lett. 39 (2014) 4719.

[35] A. Doblas, E. Sánchez-Ortiga, M. Martínez-Corral, G. Saavedra, P. Andrés, J. Garcia-Sucerquia, Shift-variant digital holographic microscopy: inaccuracies in quantitative phase imaging, Opt. Lett. 38 (2013) 1352.

Yaumel Calixto Arias Sosa was born in Manzanillo, Granma, Cuba, in 1990. He received the Bachelor degree (Best graduated in Research Topic) in Physics from the Oriente University (OU), Santiago de Cuba, Cuba, in 2014. He received the M.Sc. degree in Physics from Havana University, Havana, Cuba, in 2017. He is affiliated to the Department of Physics, OU, where he is currently working toward the Ph.D. degree in Physics. His research interests include Digital Microscopy holography, focus metrics and applications in Medicine and Biology.
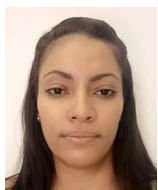
Gelaysi Moreno Vega was born in Moa, Holguín, Cuba, in 1990. She received the Bachelor degree in Physics from the Oriente University (OU), Santiago de Cuba, Cuba, in 2013. She received the M.Sc. degree in Physics from Havana University, Havana, Cuba, in 2015. She is with the Oceanographic Institute, University of São Pablo (USP), São Pablo, Brazil, where she is currently working toward the Ph.D. degree in Biological Oceanography. His research interests include Digital microscopy holography and applications in biological samples (marine plankton).

Rubens Mendes Lopes is Professor at the Biological Oceanography Department of the Oceanographic Institute, University of São Paulo. Main research interests are plankton ecology and behavior, and marine environmental monitoring. Currently leads or co-leads research projects dealing with the development and application of imaging systems and computer vision tools for automatic classification of in-situ plankton imagery. Additional research efforts in his laboratory are dedicated to understanding plankton behavioral responses using high-speed cameras and advanced optical systems.

José Luis Valin Rivera is Graduated in Mechanical Engineering from the José Antonio Echeverría Higher Polytechnic Institute in Havana, Cuba. Professor at the ISPJAE from 2007 to 2014; Master in Mechanical Engineering at the University of São Paulo (1997); PhD in Mechanical Engineering from the University of São Paulo (2001). He has worked as a Visiting Professor at the Amazonas State University (UEA) during the years (2003–2006 and 2008–2010). He is currently Professor and Director of the School of Mechanical Engineering at the Pontificia Universidad Católica de Valparaíso, Chile; Collaborator in research projects at the Technological University of Havana, Cuba; Collaborator in research projects at the Department of Mechatronics and Mechanical Systems of the Polytechnic School and the Physics Institute, both of the University of São Paulo and Collaborator in research projects at the Higher School of Technology of the Amazonas State University, Brazil. He has experience in the field of Materials and Metallurgical Engineering, with emphasis on materials and heat treatments, mainly in the following topics: Biomechanics, Materials Engineering, digital holography, Materials and Composite materials.

Edison Gonçalves is Graduated in Naval Architecture and Marine Engineering in the Escola Politecnica of Universidade of São Paulo (EPUSP), 1973, Masters in Shipping Building Technology by EPUSP, 1976, Master of Science in Ocean Engineering by Massachusetts Institute of Technology (MIT), 1980, Master of Science in Materials Science by MIT, 1980, PhD in Structural Mechanics and Materials Engineering by MIT, 1981 and Associate Professorship in Shipbuilding Technology by EPUSP, 1987. Since 1992, Full Professor in Manufacturing Engineering and Technology by University of São Paulo. He has experience in Naval Architecture and Ocean Engineering, with emphasis on Methods for the Manufacture of Ships and Ocean Systems, acting on the following subjects: mechanical manufacturing engineering, welding engineering, fracture and fatigue analysis, corrosion, residual stresses and experimental stress analysis by holographic methods. Currently has over 140 technical papers published and directly supervised 41 Master and Doctoral Thesis.

Meylí Valin Fernández is a Professor at the Department of Mechanical Engineering (DIM), Faculty of Engineering (FI), University of Concepción, Chile. Main research interest is in the mechanical characterization of composite materials with natural materials and recycled. Has a PhD in Science (2018), in the concentration area Mechanical engineering of fabrication projects, in the Mechanical Engineering Program of the Polytechnic School of the University of São Paulo (USP) (Brasil); a MSc degree in sciences with a mention on mechanical engineering (2012) from the University of Rio de Janeiro (UFRJ) (Brasil); and a bachelor's degree in mechanical engineering (2010) from the Polytechnic Superior Institute José Antonio Echeverria (ISPJAE) (Cuba).

Jorge Octavio Ricardo Pérez received the Bachelor degree in Physics Engineering from the Oriente University (OU), Santiago de Cuba, Cuba, in 1971. He received the PhD degree in Physics from UO and Saint Petersburg University, San Petersburg, Rusia. He is with the Department of Physics, OU, where he is currently Consultant Professor. His research interests include atomic and molecular Physics, digital holography, filtering, digital holography microscopy, optical processing and holographic contouring.